Accepted Manuscript

Structural performance and photothermal recovery of carbon fibre reinforced shape memory polymer

H.M.C.M. Herath, J.A. Epaarachchi, M.M. Islam, W. Al-Azzawi, J. Leng, F. Zhang

PII: S0266-3538(18)31265-X

DOI: 10.1016/j.compscitech.2018.07.042

Reference: CSTE 7328

To appear in: *Composites Science and Technology*

Received Date: 26 May 2018

Revised Date: 23 July 2018

Accepted Date: 27 July 2018

Please cite this article as: Herath HMCM, Epaarachchi JA, Islam MM, Al-Azzawi W, Leng J, Zhang F, Structural performance and photothermal recovery of carbon fibre reinforced shape memory polymer, *Composites Science and Technology* (2018), doi: 10.1016/j.compscitech.2018.07.042.

Structural Performance and Photothermal Recovery of Carbon Fibre Reinforced Shape Memory Polymer

H. M. C. M. Herath [a,b], J. A. Epaarachchi [a,b], M. M. Islam [a,b], W. Al-Azzawi [a,b], J. Leng [a,b,c], F.Zhang [c]

[a] School of Mechanical and Electrical Engineering, Faculty of Health Engineering and Sciences, University of Southern Queensland, Toowoomba, Australia

[b] Centre for Future Materials, University of Southern Queensland, Toowoomba, Australia

[c] Centre of Composite Materials and Structures, Harbin institute of Technology, Harbin, China

Corresponding Author: J. A. Epaarachchi, School of Mechanical and Electrical Engineering, Faculty of Health Engineering and Sciences, University of Southern Queensland, West Street, Toowoomba, QLD 4350, Australia, Email: Jayantha.Epaarachchi@usq.edu.au

Abstract

The shape-memory polymers (SMPs) have an interesting capability of keeping a temporary shape and then recovering the original shape when subject to a particular external stimulus. However, due to SMP's relatively low mechanical properties, the use of SMP in wider range of engineering applications is limited. As such SMP's needs to be reinforced before use in engineering applications. This paper presents the mechanical properties, thermomechanical characteristics, photothermal behaviour and light activation of 0/90 woven carbon fibre reinforced shape memory epoxy composite (SMPC) made out of prepreg material. Prepreg is widely used manufacturing technique for large-scale engineering applications. The experimental results have demonstrated that the structural performance of the SMP has increased significantly due to carbon fibre reinforcement as anticipated. According to ASTM standard D 3039/D 3039M-00, the mode of tensile failure was identified as “XMV”, where the failure is explosive type. The dynamic mechanical analysis has revealed that the shape fixity and recovery ratios of the SMPC are 100 % and 86 % respectively. Under constrained strain, the stress has been recovered up to 5.24 MPa. The SMPC was exposed to five different power densities of 808 nm and the resultant activation has been systematically investigated. Interestingly, the SMPC has been heated over its glass transition temperature, once it exposes to a power density of 1.0 W/cm^2. Furthermore, the applicability of carbon fibre reinforced SMPC for a deployable solar panel array, intended for remote and localized activation is demonstrated. The SMPC will be a potential candidate for space engineering applications, because of its enhanced mechanical properties and ability of photothermal activation.

Keywords

Functional composites, Structural composites, Carbon fibres, Thermomechanical properties, Photothermal effect

1.0 Introduction

The SMPs being evolved intensely and represent a fast growing branch of smart materials research. Since the discovery of the shape memory polymers (SMPs) in 1980s [1], the global research interest in these materials has been rapidly growing, because of their inimitable advantages of good manufacturability, high shape deformability, large recoverability, good biodegradability, and an easily tailorable glass transition temperature (Tg) [2, 3]. These advantages, make the SMPs very competitive material to replace the shape memory alloys (SMAs), which are known to have good mechanical properties, relatively expensive to manufacture and have relatively high density [4]. However, relatively low modulus and recovery stress are the inherent drawbacks of the SMPs that caused less competitive than SMAs in the past [5]. When the SMPs are reinforced with fibres (SMPCs), significant improvements have found in the mechanical properties [6]. Because of the outstanding mechanical properties, the fiber reinforced SMPCs are widely used as a structural material.

Sun et al., [7] investigated the improvement in mechanical properties that can be achieved by reinforcing the styrene-based SMP with elastic fibres. However, it is essential to investigate the effects of the reinforcement on the shape memory behavior, and the SMPC's ability to keep the temporary shape and memorize the original shape. The investigations of Al Azzawi et al, [8] on SMPCs were focused to analyze the quantitative and qualitative mechanical behavior and dimensional stability of the glass fibre reinforced styrene-based shape memory polymer composites. The results revealed that, below the glass transition temperature, the addition of glass fiber has improved the mechanical characteristics of the SMP. In addition, the SMPC have exhibited increased storage modulus compare to the neat SMP. Furthermore, the dynamic mechanical analysis (DMA) results have shown a marginal increment in the glass transition temperature in proportion to the increment of fibre to SMP ratio [8]. Fejős et al., [9] have investigated the effect of glass fibre reinforcement on the recovery behavior of the SMPC where a comparison has made between the shape memory characteristics of the Glycerol based aliphatic SMP and its glass fibres SMPC. A significant increase in the recovery stress of the SMPC has reported. However, no effect of the reinforcement on the shape recovery ratio has reported in this study as both types of materials have shown a full recovery. In the same way, the effect of carbon fibre reinforcement on the shape memory behavior has investigated by Park et al., [10] where the proposed woven carbon fibre fabric SMPC has shown a significant increase in the shape recovery rate and recovery ratio relative to the neat SMP. Gall et al., [11] have studied the deformation of carbon fiber reinforced shape memory polymer matrix composites for deployable space structure applications. The microscopic investigations has revealed that the dominant local deformation mode of the composites was buckling of the carbon fibers on the inner surface of the bend. Localized buckling out of the material plane has been lead to detrimental interfacial matrix failure while dispersed in-plane buckling was elastic and non-damaging [11]. Xie et al., [12] have developed a series of Poly (ethylene-co-vinyl acetate) (EVA) based composite with carbon fibre reinforcement (cEVA/CF). Their results revealed that cEVA/CF composites have excellent melting and crystallization capability, which were slightly affected by the incorporated carbon fibres. Furthermore, the cEVA/CF composites with 5-30 wt % CF possessed 100-650 % increase of recovery stress compared with pristine EVA. Moreover, the cEVA/CF composites exhibited a robust shape recovery performance under resistant condition, while the recovery capability of pristine cEVA was totally depressed [12].

Beside the typical heat activation, the light irradiation is more advantageous for SMP activation. Compared to heat activation, light activation enables the triggering of SMPs in a remote and localized manner with neglected intervention on surrounding circumstance [13]. The most important advantages of using light to trigger molecular processes inside materials are that, remote activation is possible since light can travel a long distance, spatially controlled activation is possible as the light beam (often a laser) can be delivered to selected areas and light-triggered processes can be halted and resumed ‘‘on-demand’’ by turning on-off or controlling the power of the excitation light [14]. Lu et al., [15] found that a unique synergistic effect of CNTs and boronnitride which could facilitate the thermally conductive and accelerate the infrared light induced shape recovery behaviour of the SMP nanocomposites. Gold nanoparticles (AuNPs) and nanorods (AuNRs) attract more attention for absorbing light at their surface plasmon resonance (SPR) wave lengths and thus generating heat release [16]. Two cost efficient fillers, based on the rare earth organic complexes of Yb(TTA)3Phen and Nd(TTA)3Phen, demonstrate selectively photo thermal effect to near infrared (NIR) light of 980 nm and 808 nm, respectively [13]. Exposure of human skin tissues and naked eyes to NIR light is safer. Due to this reason NIR light has been widely used to trigger intelligent SMPCs containing carbon nanomaterials, metal nanoparticles, or rare earth organic complexes [17]. Fang et al., [17] has used $NaYF_4$:99.5%Yb^{3+}, 0.5%Tm^{3+} particles as multifunctional fillers to achieve both upconversion and photothermal effects. The upconversion effect is useful to detect the position of laser beam on SMPC surface at a relatively low power density [17].

SMPs are inherently a weaker polymeric material. For this reason, the significance of SMP composites (SMPCs) have been analysed in terms of four aspects: reinforcement, innovation and improvement of driving methods, the creation of specific deformations and the creation of multifunctional materials [18]. This paper predominantly presents the experimental investigations on material structure, mechanical properties and thermo-mechanical behavior of 0/90 woven carbon fibre reinforced shape memory epoxy composite made out of prepreg material. Prepreg is widely used manufacturing technique for large-scale engineering applications, because of its advantages such as provision of set weight characteristics and improvement of the work procedure during molding of items from polymeric composite materials [19]. Moreover, the competency of the carbon fibres as a reinforcing material, photothermal filler and thermal conductor has been exclusively investigated. The SMPC was exposed to five different power densities of 808 nm and the activation in a remote and localized manner has been systematically investigated. Because of its enhanced mechanical properties and ability of photothermal activation, SMPC will be a potential candidate for space engineering applications. Furthermore, the applicability of carbon fibre reinforced SMPC for a deployable solar panel array intended for remote and localized activation is demonstrated. In addition, this paper conceptually demonstrates that the high strength structures made from SMPCs can be compressed and packed in a spacecraft, transported to an outer space location and ultimately deployed in to the expanded shape by NIR radiation.

2.0 Material and experimental methods

2.1 Material

Based on the reinforced phase, SMPCs can be primarily classified into two types called particulate reinforced composites and fibre reinforced composites. Interestingly, the particulate reinforced composites have high recovery stress and recovery strain. However, their mechanical properties are relatively poor. Therefore, the fibre reinforced SMPCs are widely used as a structural material because of their relatively higher mechanical properties [20]. Interestingly, the carbon fibre reinforced SMPCs can exhibit a robust shape recovery performance under resistant condition [12]. The SMPCs are subjected to heating during its operation, which affects to the dimensional stability of the components [8]. Furthermore, the SMPCs can be subjected to shear during its operation. Advantageously, the 0/90 woven fibre reinforcement is useful to overcome such problems [21, 22]. Carbon fibre reinforced shape memory epoxy prepreg, which was supplied from the Harbin Institute of Technology - China, has been used to prepare the samples. Four laminations of prepreg sheets containing 0/90 woven plain fibre mesh were cured with vacuum bagging under 70 bar for 9 hours at 80 ^{o}C, 100 ^{o}C and 150 ^{o}C respectively with equal time spacing. The formed sheets were cut in to rectangle shapes by using the diamond saw cutter. The specification of the test specimens used for each experiment is illustrated in Table 1

.

Table 1. Specification of the SMPC test specimens and respective experiment

Experiment	Dimension (mm)			No of layers	No of test specimens
	Length	Width	Thickness		
DMA tests	35.0	8.0	1.1	04	03
Tensile test	270.0	15.0	1.2	04	05
Compression test	140.0	12.8	1.2	04	05
Impact test	100.0	12.0	1.2	04	05
Photothermal behaviour	150	150	1.2	04	01
Light activated shape recovery	35.0	8.0	1.2	04	05

The Shimadzu Fourier Transform Infrared Spectrometer (IRAffinity-1S FTIR) has been used to obtain the infrared spectrum of transmittance of the prepared samples. The layer formation and the surface quality of the samples have been observed, by using the Jeol Benchtop Scanning Electron Microscope (JCM-6000 SEM).

2.2 Dynamic mechanical analysis

TA instruments dynamic mechanical analyzer (DMA Q800) with a double cantilever clamp has been used to investigate the thermo-mechanical behaviour of the SMPC. The multi-frequency strain mode has been used to determine the glass transitions temperature (T_g) and to characterize the storage modulus, by using a frequency of 1 Hz and temperature ramp of 5 °C/min from 55 °C to 120 °C. In addition, the stress-free strain recovery and constrained strain stress recovery characteristics of the material have been investigated. For both experiments, the shape programing has been carried out by using the following DMA programme. Under the DMA strain rate mode, the initial temperature and strain were set to 30 °C and 0 % respectively. The shape programing phase was started with a temperature ramp of 5 °C/min up to 130 °C with zero strain, continued by a constant temperature of 130 °C for 7 min with an intermediate strain ramp of 0.5 %/min up to 1.5 % strain. Next, the specimen was cooled with a temperature ramp of 5 °C/min down to 30 °C while keeping the 1.5 % constant strain. Subsequently, the specimen was kept at a constant temperature of 30 °C for 15 min and the constrain was released where the temporary fixed shape was achieved. The stress-free strain recovery has been investigated under DMA strain rate mode. The specimen was subjected to a temperature ramp of 5 °C/min up to 130 °C and isothermal for 20 min where the strain recovery was observed. Moreover, the constrained strain stress recovery has been investigated under the DMA iso-strain mode with a constant strain of 1.5 %. The specimen was subjected to a temperature ramp 5 °C/min up to 130 °C and isothermal for 20 min, where the stress recovery has been observed.

2.3 Tensile, compression, impact and hardness tests

The mechanical properties of the material have been examined to ensure to structural performance in a robust condition. MTS 100 kN, Insight Electromechanical Testing Systems has been used for the tensile testing under ISO 527-5:2009 standards [23]. Furthermore, under ASTM D6641 standards [24], compression testing for SMPC was carried out on the same MTS testing machine. The impact testing has been performed by using Instron Dynatup Drop Weight Impact Testing Instrument (8200). Barcol Impressor Hand-held portable hardness tester (GYZJ-934-1) has been used to determine the hardness of the composite polymer material. All the experiments have been conducted at the room conditions.

2.4 Photothermal behaviour

By using the FLIR A65 Thermal Imaging Camera, the photothermal behaviour of the carbon fibre reinforced SMPC has been investigated for five different power densities (0.01, 0.5, 1.0, 1.5 and 2.0 W/cm^2) of 808 nm near infrared radiation.

2.5 Light activated shape memory behaviour

The light activated shape recovery of the SMPC has been investigated experimentally. The specimens were heated up to 130 °C by using the oven and programed in to the 90° bending, followed by natural cooling up to room temperature to fix the shape. Subsequently the specimens were exposed to five different power densities 0.01, 0.5, 1.0, 1.5 and 2.0 W/cm^2 of 808 nm near infrared radiation and recovery angles were video recorded by using the Nikon D3400 DSLR camera. Furthermore, by using the Gwyddion open source image analysis software, the recovery angles were measured. In addition, competency of the developed SMPC for a space engineering application has been investigated. A model of a deployable solar panel array has been fabricated by using four Sanyo Amorphous Solar Cell Photovoltaic Solar Panels (58.1 x 48.6 x 1.3 mm) supplied by the RS Components, Australia. The solar panels were coupled and hold by SMPC structural members (50 x 10 x 1.2 mm). The SMPC structural members were heated above T_g and programed in to a compact shape. Subsequently, it has been recovered in to the fully expanded shape by following four steps of localised NIR irradiation (808 nm, 2 W/cm^2).

3.0 Results and discussion

3.1 Material characteristics

Polymers are compounds consisting of extremely long chains of atoms where the epoxy resins are a family of thermosetting materials widely used as adhesives or matrices in polymer composites. Epoxy thermosets can be described as 3D polymer networks formed by the chemical reaction between monomers where complex geometries can be easily shaped and fixed after curing the monomers. The SMPC test specimens were produced by vacuum curing and ~18 % of mass reduction has been recorded during the process. This has happened due to the absorption of resin by the bleeder layer which were flowed through the peel ply.

Finally, the samples consisted with ~30 % of mass fraction of carbon fibre. The infrared spectrum of transmittance for the produced SMPC is shown in Fig 1 and Table 2 describes the relevant assignments of the FTIR absorption peaks. The interpretation of the IR spectra and the assignment of the FTIR bands are significant in monitoring the curing process, phase separation and ageing. However, beyond the general use of FTIR, the spectrum of IR absorption (invert of transmittance spectrum) gives indications on energizing the material by infrared rays. According to the FTIR results shown is Fig. 1, the SMPC has several absorption peaks from 3422 nm (2922 cm^{-1}) to 18116 nm (552 cm^{-1}). Therefore, there is a possibility for photothermal heating by mid-range infrared radiation as well.

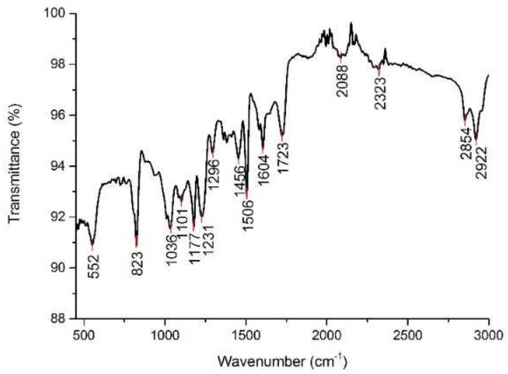

Fig. 1. Infrared spectrum of transmittance for SMPC

Table 2. Assignments for major FTIR transmittance bands for SMPC

Band (cm^{-1})	Assignment
823 [25]	Stretching C-O-C of oxirane group
1036 [25]	Stretching C-O-C of ethers
1506 [25]	Stretching C-C of aromatic
1604 [25]	Stretching C=C of aromatic rings
1723 [26]	Stretching free C=O amide I
2700-3000 [25]	Stretching C-H of CH and CH aromatic and aliphatic

In addition, scanning electron microscopy has provided more information on surface features and delamination. Fig. 2a illustrate the SEM image of the top surface appearance. Accordingly, at few locations of the top surface, voids were appeared with lengths ranging up to 205 μm. Fig. 2b illustrates the cross-section. Accordingly there are micro level gaps in between prepreg layers throughout the thickness. The maximum gap in between two prepreg layers was measured as 32.4 μm. Furthermore, the SEM image Fig. 2c demonstrates the porous areas in the material. Fig. 2d illustrates the 0/90 woven fibre mesh and the diameters of the fibres. Accordingly, the average diameter of the carbon fibres used in this research is 14 μm.

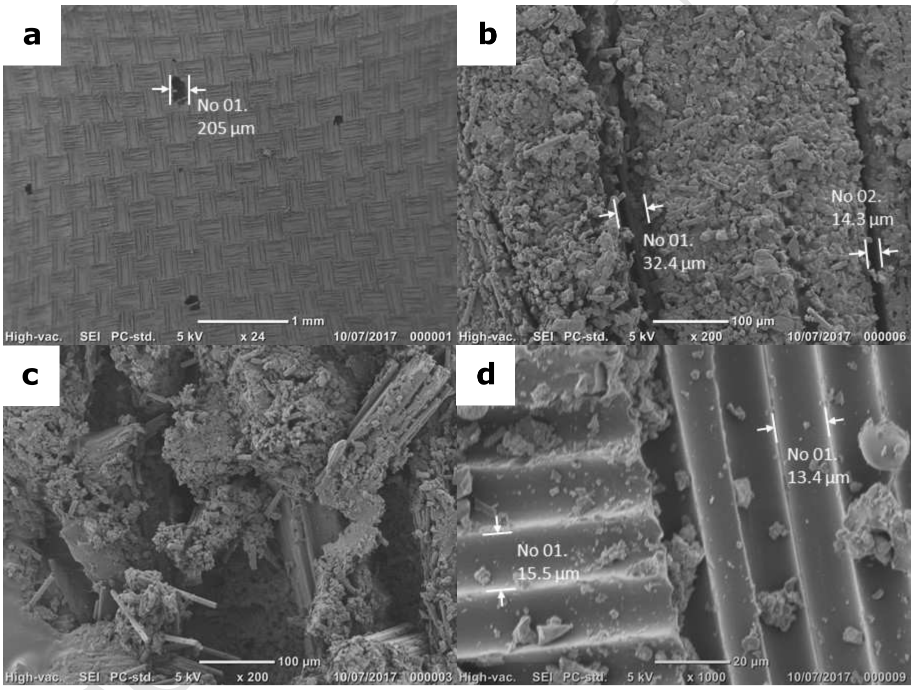

Fig. 2. SEM images (a) voids on top surface (b) gaps between layers (c) porous area on cross-section (d) 0/90 woven fibre mesh

3.2 Mechanical properties

The stress strain curves for tensile and compression tests are shown in Fig. 3a and Fig. 3b respectively. Calculated tensile strength of the SMPC is 547 MPa and the elastic modulus is 52 GPa. The tensile strength of the SMPC has increased by 10 folds compare to neat SMP.

Moreover, the compressive strength of the SMPC is 120 MPa which is a significant improvement. Stress-strain behaviour under tensile and compressive loads has shown a non-linear trend. Both tensile and compression stress-strain curves have been fitted for second order polynomial curves. The reason for such behaviour might be the voids between laminae and progressive failures of fibres due to local bending at void locations [27]. By compare to the tensile and compression properties of general thermoset polymers (Polyester resin, Vinyl ester resin, Epoxy) the carbon fibre reinforced shape memory epoxy has demonstrated an outstanding tensile strength and the compressive strength of the SMPC remains in the typical range for general thermosets [28].

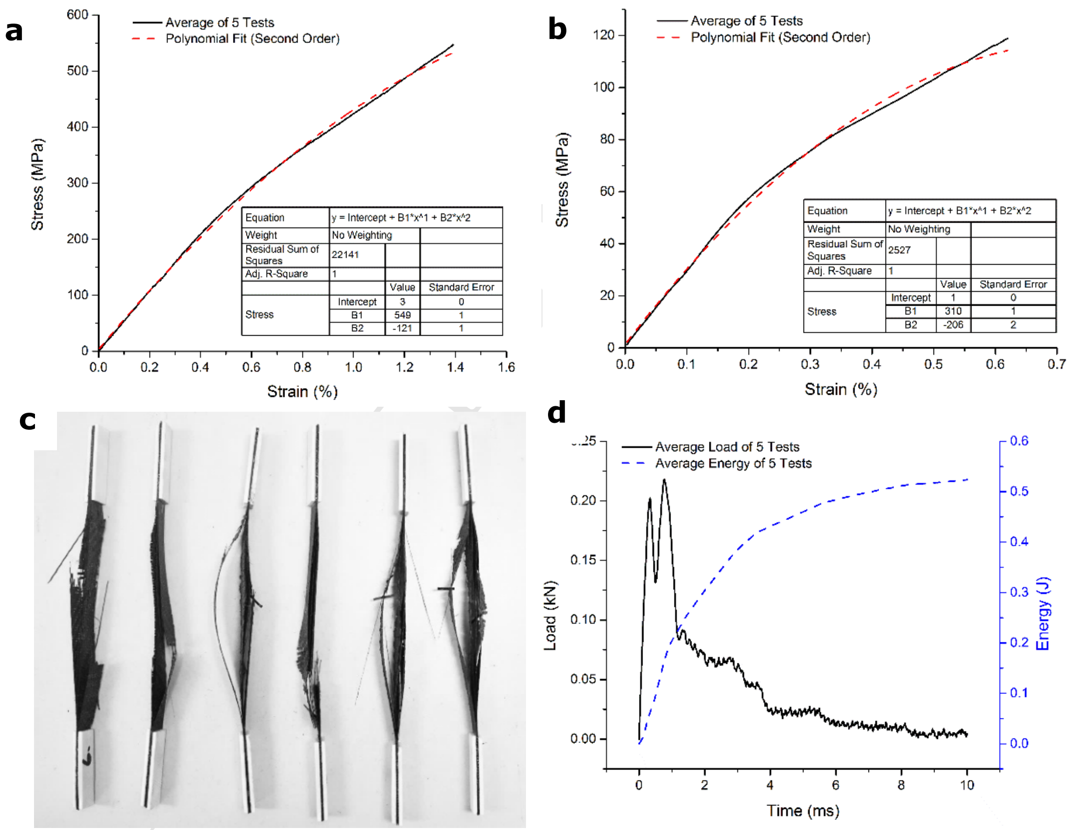

Fig. 3. Mechanical properties of the SMPC (a) tensile stress versus strain (b) compression stress versus strain (c) delamination occurred during the tensile failure (d) impact load, energy versus time

However, as illustrated in Fig. 3c, at the point of tensile failure, a delamination of the material has been noticed. According to the ASTM Standard D 3039/D 3039M-00 [29], the mode of tensile failure can be categorized as "XMV" where the failure is explosive type, in multiple areas and in various locations. However, the tensile experiments carried out by Paiva et al., [30] for carbon fabric (0/90) reinforced epoxy composites have showed that, the failure of specimen has followed lateral type brittle failure. Furthermore, based on the epoxy, the failure location has been varied as, inside grip, at grip, gage or multiple area. Importantly, none of the specimens of Paiva et al.,[30] were broken under "XMV" mode. Possibly the micro level delamination between the layers which are identified during the SEM examinations might have caused local bending to propagate micro delamination until the failure of SMPC [27, 31]. The impact energy absorbance of the SMPC is illustrated in Fig. 3d. The measured fracture energy of the tested samples was 0.54 J. Furthermore, the hardness of the SMPC which was measured in Barcol Impressor scale is 56, which is approximately 39 in Brinnell and 44 in Vickers scales. Table 3 presents the summary of physical and mechanical properties of the SMP epoxy composite comprising ~30 % mass fraction of carbon fibres. All the mechanical tests were conducted at the room conditions.

Table 3. Physical and mechanical properties of carbon fibre reinforced SMP epoxy

Property	Value	Unit
Density	1.3	g/cm^3
Tensile strength	547	MPa
Elastic modulus	52	GPa
Compressive strength	120	MPa
Impact energy	0.54	J
Hardness	56	Barcol Impressor

3.3 Thermomechanical behaviour

The storage modulus, loss modulus and tan delta curves for the SMPC are presented in Fig. 4. The onset point of the storage modulus curve, peak of the loss modulus curve or the peak of the tan delta curve are often employed to define the glass transition temperature (T_g). However, here the T_g is defined by considering the onset point of the storage modulus curve. Accordingly, the T_g of the SMPC with ~30 % mass fraction of carbon fibre was determined as 80 ^oC. Incorporated carbon fibres has influenced to increase the T_g by 10 ^oC compared to neat SMP [8]. By considering the material parameters defined by Baghani et al., [32] the temperatures T_l, T_g and T_h can be identified as 60 ^oC, 80 ^oC and 100 ^oC respectively [8]. When the temperature is at T_l, T_g, and T_h, the material is at dominant frozen phase, combination of both phases and dominant active phase respectively [32]. Therefore, the temperature region T_l to T_h can be defied as the transition region of the material where the shape recovery takes place [8].

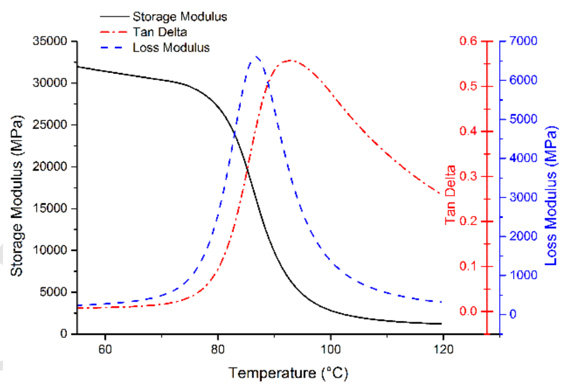

Fig. 4. Storage modulus, loss modulus and tan delta verses temperature

The strain recovery curve obtained from DMA, under strain rate mode has shown the shape memory characteristics of the SMPC. As per the illustration on Fig. 5a, no spring back effect has shown after the shape programing phase, because the fixed temporary shape and the required temporary shape is equal. Moreover, it indicates that the strain recovery begins at

62 °C and recovers from 1.5 % to 0.12 % after the temperature ramp up to 130 °C, followed by a constant temperature for 20 min. However, the original strain was 0%. Referring to the definitions by Fejős et al., [9] it can be quantified that the SMP epoxy with ~30 % mass fraction of carbon fibre has shown excellent shape fixity ratio of almost 100 % and the shape recovery ratio of 86 %. Fig. 5b depicts the behaviour of the SPMC under constrained strain recovery condition. Due to strain increment at programing phase the stress has been increased up to 7.47 MPa, followed by a decrease until 0.04 MPa due to the stress relaxation effect within the shape programming stage. The reason behind such stress relaxation, is the high viscoelastic behaviour of the material at the elevated temperature. In the recovery phase, the stress recovery started at almost 62 °C and recovered up to 5.24 MPa after the temperature ramp up to 130 °C, followed by a constant temperature for 20 min.

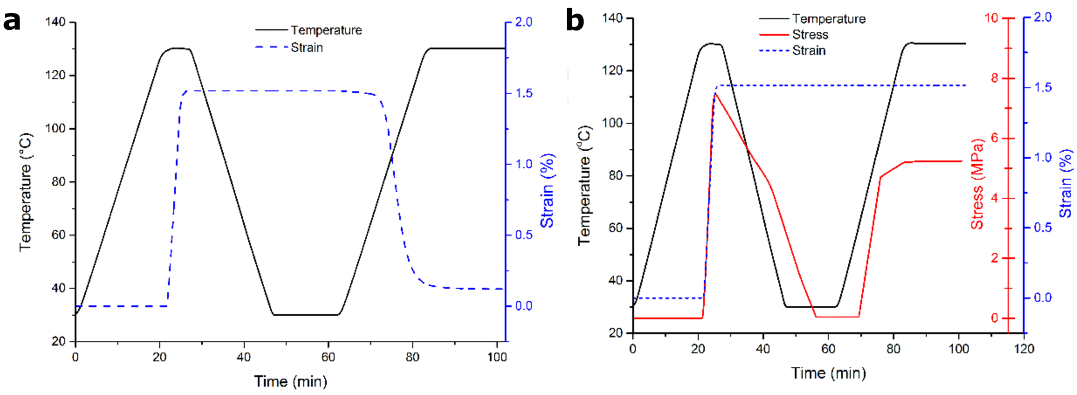

Fig. 5. Full thermomechanical cycles (a) shape programming and stress-free strain recovery process (b) shape programming and constrained strain stress recovery process

3.4 Photothermal behaviour

The photothermal effect is a phenomenon which produce the thermal energy from electromagnetic radiation. Once the electromagnetic radiation is absorbed by a material, free electrons of the material will vibrate at very high frequency, and reach higher energy levels. Part of the vibrational energy is converted into the electromagnetic waves and radiate outwards. The rest is transformed into kinetic energy of electrons and then converted into heat energy through the relaxation process between electrons and lattices. The shape memory polymer composites exposed to light radiation can perform shape recovery once it is heated above its T_g due to the photothermal effect. The photothermal behaviour of the carbon fibre, neat epoxy and SMPC have been investigated for five different power densities of 0.01, 0.5, 1.0, 1.5 and 2.0 W/cm^2 of 808 nm near infrared radiation. The specimens were exposed to the 808 nm radiation of a 10 mm diameter circular area. Fig. 6a shows the temperature recorded area by using the FLIR A65 thermal imaging camera. The centre of the laser is denoted by "O" and by considering the centre as the origin XY Cartesian coordinates are defined. The average temperature of a 3 x 3 pixel area at the origin were recorded for 120 seconds for all five power densities. It has been noticed that the origin of the carbon fibre and SMPC specimens were heated up to a particular temperature and be constant at that temperature thorough out the time. The reason for such behaviour is the radiation of electromagnetic waves due to higher energy levels of the electrons. Moreover, there is a heat transfer from the laser exposed area to unexposed areas of the material. Fig. 6b illustrates the temperature increment at the origin for carbon fibre and neat epoxy. Accordingly, the neat epoxy has showed slight increment in temperature due to the 808 nm radiation. However, the carbon fibre has shown a significant photothermal effect and heated up to 183 ^oC at the power density of 2.0 W/cm^2. Furthermore, the carbon fibres exposed to NIR radiation demonstrated a rapid increment of temperature and reached the stabilised temperature in few seconds. Such temperature increment has been noticed only for the carbon fibres, because once exposed to NIR radiation the free electrons on the outer surface vibrate at very high frequency and reach higher energy levels. In essence, the thermal imaging camera detects the surface temperature. For the carbon fibre, there is no liner relationship between the highest temperature and power density. With the increment of power density the gaps between the highest temperatures are getting close. The reason for this might be the reflectance of NIR radiation by the exposed surface. Fig. 6c illustrates the photothermal behaviour of SMPC. Compared to carbon fibres, SMPC has demonstrated a slow temperature increase rate, because the surface of the SMPC samples are covered with epoxy and the epoxy's low heat conductivity has delayed the transfer of the heat generated by the carbon fibres to the outer surface. Also, the SMPC has reached for higher temperatures with respect to the increase of power density. The less reflectance of NIR radiation by the exposed surface of SMPC which contains the epoxy might have caused for this. Furthermore, with compare to the carbon fibres, SMPC has taken longer time to reach its highest temperature, because the SMP epoxy has been heated by the incorporated carbon fibres. Fig. 6d illustrates the temperate along the X direction after being exposed 120 seconds, where X zero is the centre of the laser exposed area (origin). The highest temperature is at the origin and reduces along the X axis and reaches almost the room temperature after 40 mm distance from the origin. This demonstrates the capability of using NIR light for localized activation of SMPCs, where a particular area around the laser centre is heated above its T_g. Furthermore, the radius of the area which reaches a temperature above T_g can be controlled by changing the power density of the laser. As illustrated in Fig. 6d, when SMPCs are exposed to a power density of 1.0, 1.5 and 2.0 W/cm^2, the radius of the area which reaches a temperature above T_g has been determined as 7.5, 10.5 and 12.5 mm respectively.

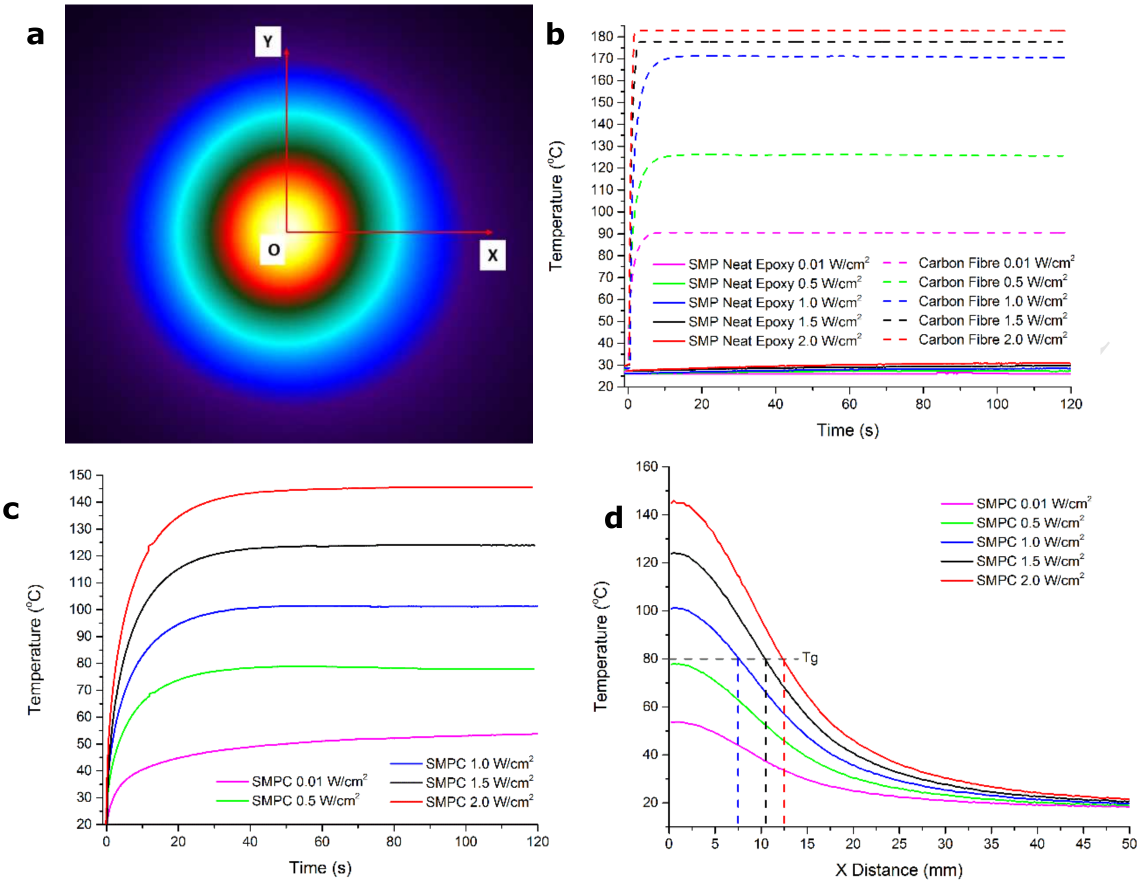

Fig. 6. Photothermal behaviour due to 808 nm irradiation (a) temperature recorded area and the centre of the laser exposed area (b) temperature increment at the origin for carbon fibre and neat epoxy (c) temperature increment at the origin for SMPC (d) temperature of SMPC along the X direction after being exposed for 120 seconds

3.5 Light activated shape memory behaviour

The light activated shape recovery of the SMPC has been investigated experimentally. 90^{o} bended SMPC specimens were exposed 808 nm near infrared radiation and recovery angles were observed. Fig. 7a-d illustrate the respective shape recovery steps of the SMPC, starting from the initial stage with 90^{o} bend, two intermediate recovery stages and the final stage showing almost full recovery. Furthermore, by using the Gwyddion open source image analysis software the recovery angles were measured for 21 seconds with 3 second gaps and presented in Fig. 8. Accordingly, the specimen, which was exposed 2.0 W/cm^{2} power density, has started the shape recovery soon after the exposure to laser radiation. Recovery starting point of the other three specimens have been delayed with respect to the reduction of power density. The reason for this is the time taken to transfer the heat in to the bottom layers of the SMPCs with 1.2 mm thickness. The specimens exposed to 2.0, 1.5, and 1.0 W/cm^2 have been almost fully recovered after being exposed to 12, 18 and 21 seconds respectively, which means the recovery rate depends on the power density. Increment of the power density increases the recovery rate. The specimen exposed to 0.5 W/cm^2 power density has been reached a 150^o recovery angle in 21 seconds. It has been noticed that the sample was fully recovered after being exposed to 78 seconds of continued laser radiation with 0.5 W/cm^2 power density. According to the Fig. 6c, the specimen exposed to 0.5 W/cm^2 should reach only 78 ^{o}C which is less than the glass transition temperature determined from Fig. 4. However, as described in section 3.3 the specimen exposed to 0.5 W/cm^2 has reached the transition region (T_l-T_h) and was able to accomplish a shape recovery. As illustrated in Fig. 6c, the specimen exposed to 0.01 W/cm^2 has heated to 54 ^{o}C, which is less than T_l. Therefore, the specimen exposed to 0.01 W/cm^2 has not shown any shape recovery behaviour.

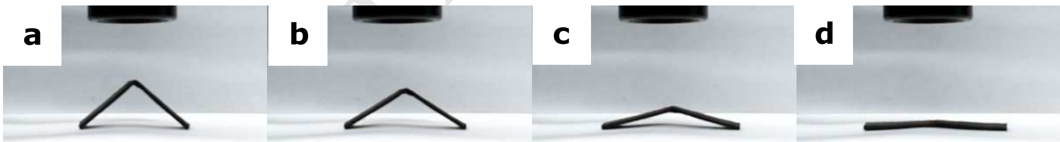

Fig. 7. 808 nm light activated shape recovery steps for SMPC (a) initial stage with ~90^o bend angle (b) intermediate stage one with ~115^o recovery angle (c) intermediate stage two ~150^o recovery angle (d) final stage with ~173^o recovery angle

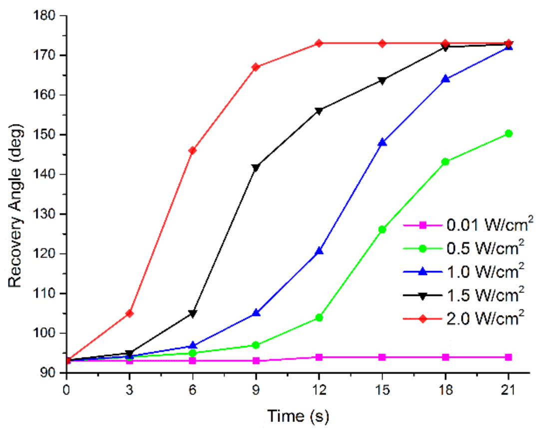

Fig. 8. 808 nm light activated shape recovery angles verses time for SMPC

Fig. 9, illustrates a model of a deployable solar panel array, which can be used in a satellite. Fig 9a, shows the sectional view of the initial compacted shape and the areas subjected to NIR radiation (808 nm, 2 W/cm^2) during the four steps of localized activation. Furthermore, the anticipated shape recovery behaviour of the each step is shown by the arrows. The compacted and programmed shape of the deployable solar panel array is illustrated in Fig. 9b. Successively, Fig 9c, d and e present the appearance of the partially recovered solar panel array after the activation step 1, 2 and 3 respectively. In each case, the number of solar panels in use is different and it is increasing correspond to the activation steps. The final and fully expanded solar panel array with all four solar panels in use is presented in Fig 9f. Endures uniquely in harsh environment and maintaining the structural permanence are the most challenging concerns on selecting lightweight materials for space applications [33]. Also, the development of deployable structures becomes important as it reduce the occupied room in spacecraft and make the best use of the deployed volume in space [34]. Therefore, the carbon fibre reinforced SMPCs can be used to produce deployable solar panel arrays for satellites which can be compressed and packed in a spacecraft, transported to an outer space location and ultimately deployed in to the expanded shape by NIR radiation.

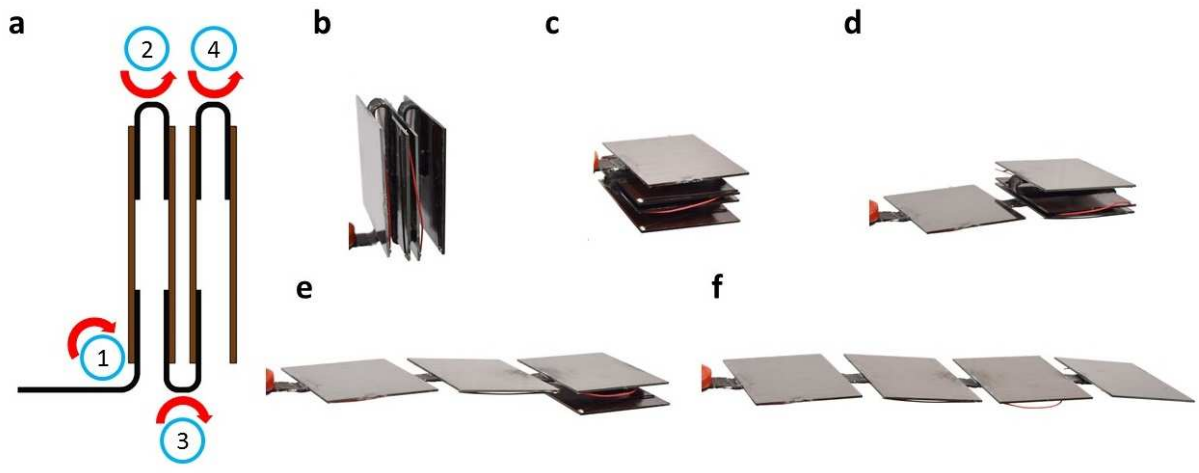

Fig. 9. Model of a deployable solar panel array for a satellite (a) steps of NIR irradiation and respective shape recovery behaviours (b) primary compacted shape (c) view after recovery step 01, one solar panel in use (d) view after recovery step 02, two solar panels in use (e) view after recovery step 03, three solar panels in use (f) fully recovered view after step 04, four solar panels in use.

4.0 Conclusion

This paper presents the mechanical properties, thermomechanical characteristics and photothermal behaviour of the carbon fibre reinforced shape memory. The porous areas which were identified through the thickness of the SMPC specimens might be the reason for non-linear stress strain behaviour observed during the tensile and compression experiments. Furthermore, the micro level delamination between the layers might have caused local bending to propagate micro delamination until the failure. This observation suggests the necessity of appropriate pressure and resin flow during the curing of SMP prepreg, which should be researched further. However, the presence of carbon fibre has exhibited superlative enhancement in mechanical strength. The tensile strength of the SMPC has increased by 10 times compare to the neat SMP epoxy. Interestingly, the SMPC with carbon fibre has exhibited an excellent shape memory behaviour without any spring back effect and 86 % strain recovery. In addition to the use of carbon fibres as a reinforcing material, it can be used as a photothermal filler which is trigged to 808 nm NIR radiation. Moreover, NIR radiation can be used to accomplish remote controlled and localized activation of SMPCs, which is impossible with typical thermal activation. The SMPC has been heated over its glass transition temperature under the direct exposer to 808 nm near infrared laser with 1.0 W/cm^2. The temperature of the SMPC has been increased with respect to the increase of power density of 808 nm laser. Moreover, the light activation experiments have revealed that the recovery staring time and recovery rate also depend on the power density of the 808 nm laser. Because of its enhanced mechanical properties and ability of photothermal activation, SMPC will be a potential candidate for space engineering applications. It can be concluded that, the carbon fibre reinforced SMPCs can be used to produce deployable space applications which can be compressed and packed in a spacecraft, transported to an outer space location and ultimately deployed in to the expanded shape by NIR radiation. However, further studies on manufacturing of such SMPC components are warranted.

Acknowledgement

The authors are indebted to the Harbin Institute of Technology, China, for providing help and material used in this work.

Funding

This work was supported by the Asian Office of Aerospace Research and Development (AOARD), Air Force Office of Scientific Research (AFOSR), U.S. Air Force [grant number FA2386-16-1-4043].

References

[1] Y. Liu, H. Lv, X. Lan, J. Leng, S. Du, Review of electro-active shape-memory polymer composite, Composites Science and Technology 69(13) (2009) 2064-2068.
[2] J. Leng, X. Lan, Y. Liu, S. Du, Shape-memory polymers and their composites: stimulus methods and applications, Progress in Materials Science 56(7) (2011) 1077-1135.
[3] W. Al Azzawi, J.A. Epaarachchi, M.M. Islam, J. Leng, Shape memory polymers and their applications, Structural health monitoring technologies and next-generation smart composite structures, Taylor & Francis (CRC Press)2016, pp. 447-478.
[4] R. DesRoches, B. Smith, Shape memory alloys in seismic resistant design and retrofit: a critical review of their potential and limitations, Journal of Earthquake Engineering 8(03) (2004) 415-429.
[5] E.R. Abrahamson, M.S. Lake, N.A. Munshi, K. Gall, Shape memory mechanics of an elastic memory composite resin, Journal of intelligent material systems and structures 14(10) (2003) 623-632.
[6] T. Ohki, Q.-Q. Ni, N. Ohsako, M. Iwamoto, Mechanical and shape memory behavior of composites with shape memory polymer, Composites Part A: applied science and manufacturing 35(9) (2004) 1065-1073.
[7] J. Sun, Y. Liu, J. Leng, Mechanical properties of shape memory polymer composites enhanced by elastic fibers and their application in variable stiffness morphing skins, Journal of Intelligent Material Systems and Structures 26(15) (2015) 2020-2027.
[8] W. Al Azzawi, M.M. Islam, J. Leng, F. Li, J.A. Epaarachchi, Quantitative and qualitative analyses of mechanical behavior and dimensional stability of styrene-based shape memory composites, Journal of Intelligent Material Systems and Structures (2017) 1-12.
[9] M. Fejős, G. Romhány, J. Karger-Kocsis, Shape memory characteristics of woven glass fibre fabric reinforced epoxy composite in flexure, Journal of Reinforced Plastics and Composites 31(22) (2012) 1532-1537.
[10] J.-M. Park, D.-J. Kwon, Z.-J. Wang, J.-U. Roh, W.-I. Lee, J.-K. Park, K. Lawrence DeVries, Effects of carbon nanotubes and carbon fiber reinforcements on thermal conductivity and ablation properties of carbon/phenolic composites, Composites Part B: Engineering 67(Supplement C) (2014) 22-29.
[11] K. Gall, M. Mikulas, N.A. Munshi, F. Beavers, M. Tupper, Carbon Fiber Reinforced Shape Memory Polymer Composites, Journal of Intelligent Material Systems and Structures 11(11) (2000) 877-886.
[12] H. Xie, L. Li, X.-Y. Deng, C.-Y. Cheng, K.-K. Yang, Y.-Z. Wang, Reinforcement of shape-memory poly(ethylene-co-vinyl acetate) by carbon fibre to access robust recovery capability under resistant condition, Composites Science and Technology 157 (2018) 202-208.
[13] L. Fang, S. Chen, T. Fang, J. Fang, C. Lu, Z. Xu, Shape-memory polymer composites selectively triggered by near-infrared light of two certain wavelengths and their applications at macro-/microscale, Composites Science and Technology 138 (2017) 106-116.
[14] D. Habault, H. Zhang, Y. Zhao, Light-triggered self-healing and shape-memory polymers, Chemical Society Reviews 42(17) (2013) 7244-7256.
[15] H. Lu, Y. Yao, W.M. Huang, J. Leng, D. Hui, Significantly improving infrared light-induced shape recovery behavior of shape memory polymeric

nanocomposite via a synergistic effect of carbon nanotube and boron nitride, Composites Part B: Engineering 62 (2014) 256-261.
[16] H. Zhang, Y. Zhao, Polymers with Dual Light-Triggered Functions of Shape Memory and Healing Using Gold Nanoparticles, ACS Applied Materials & Interfaces 5(24) (2013) 13069-13075.
[17] L. Fang, T. Fang, X. Liu, Y. Ni, C. Lu, Z. Xu, Precise stimulation of near-infrared light responsive shape-memory polymer composites using upconversion particles with photothermal capability, Composites Science and Technology 152 (2017) 190-197.
[18] T. Mu, L. Liu, X. Lan, Y. Liu, J. Leng, Shape memory polymers for composites, Composites Science and Technology 160 (2018) 169-198.
[19] N.I. Baurova, V.A. Zorin, Current prepreg-formation technologies, Polymer Science, Series D 10(2) (2017) 156-159.
[20] J. Guo, Z. Wang, L. Tong, H. Lv, W. Liang, Shape memory and thermo-mechanical properties of shape memory polymer/carbon fiber composites, Composites Part A: Applied Science and Manufacturing 76 (2015) 162-171.
[21] J. Cao, R. Akkerman, P. Boisse, J. Chen, H.S. Cheng, E.F. de Graaf, J.L. Gorczyca, P. Harrison, G. Hivet, J. Launay, W. Lee, L. Liu, S.V. Lomov, A. Long, E. de Luycker, F. Morestin, J. Padvoiskis, X.Q. Peng, J. Sherwood, T. Stoilova, X.M. Tao, I. Verpoest, A. Willems, J. Wiggers, T.X. Yu, B. Zhu, Characterization of mechanical behavior of woven fabrics: Experimental methods and benchmark results, Composites Part A: Applied Science and Manufacturing 39(6) (2008) 1037-1053.
[22] S. Ekşi, K. Genel, Comparison of Mechanical Properties of Unidirectional and Woven Carbon, Glass and Aramid Fiber Reinforced Epoxy Composites, ACTA PHYSICA POLONICA A 132 (2017) 879-882.
[23] ISO 527-5:2009, Plastics - Determination of tensile properties - Part 5: Test conditions for unidirectional fibre-reinforced plastic composites, International Organization for Standardization, 2009-07.
[24] ASTM D6641 / D6641M-16e1, Standard Test Method for Compressive Properties of Polymer Matrix Composite Materials Using a Combined Loading Compression (CLC) Test Fixture
ASTM International, West Conshohocken, PA, 2016.
[25] M.G. González, J.C. Cabanelas, J. Baselga, Applications of FTIR on epoxy resins-identification, monitoring the curing process, phase separation and water uptake, Infrared Spectroscopy-Materials Science, Engineering and Technology, InTech2012, pp. 261-284.
[26] C. Guignot, N. Betz, B. Legendre, A. Le Moel, N. Yagoubi, Degradation of segmented poly (etherurethane) Tecoflex® induced by electron beam irradiation: characterization and evaluation, Nuclear Instruments and Methods in Physics Research Section B: Beam Interactions with Materials and Atoms 185(1) (2001) 100-107.
[27] A.A. Kakei, M. Islam, J. Leng, J.A. Epaarachchi, Use of an elasto-plastic model and strain measurements of embedded fibre Bragg grating sensors to detect Mode I delamination crack propagation in woven cloth (0/90) composite materials, Structural Health Monitoring (2017) 1-16.
[28] H. Ku, H. Wang, N. Pattarachaiyakoop, M. Trada, A review on the tensile properties of natural fiber reinforced polymer composites, Composites Part B: Engineering 42(4) (2011) 856-873.
[29] ASTM D3039/D 3039M, Standard test method for tensile properties of polymer matrix composite materials, ASTM International, West Conshohocken, PA, 2008.

[30] J.M.F.D. Paiva, S. Mayer, M.C. Rezende, Comparison of Tensile Strength of Different Carbon Fabric Reinforced Epoxy Composites, Materials Research 9(1) (2006) 83-89.
[31] A.A.G. Kakei, J.A. Epaarachchi, M.M. Islam, Development of fracture and damage modeling concepts for composite materials, Structural health monitoring technologies and next-generation smart composite structures, CRC Press2016, pp. 339–364.
[32] M. Baghani, R. Naghdabadi, J. Arghavani, S. Sohrabpour, A constitutive model for shape memory polymers with application to torsion of prismatic bars, Journal of Intelligent Material Systems and Structures 23(2) (2012) 107-116.
[33] L. Yanju, D. Haiyang, L. Liwu, L. Jinsong, Shape memory polymers and their composites in aerospace applications: a review, Smart Materials and Structures 23(2) (2014) 023001.
[34] L. Xin, L. Yanju, L. Haibao, W. Xiaohua, L. Jinsong, D. Shanyi, Fiber reinforced shape-memory polymer composite and its application in a deployable hinge, Smart Materials and Structures 18(2) (2009) 024002.